

# Ultrasound Evaluation of Soft Tissue Masses and Parotid Gland in Clinical Rheumatology

Hèctor Corominas<sup>1</sup>, Delia Reina<sup>2</sup>, Vanessa Navarro<sup>2</sup>, Oscar Camacho<sup>2</sup>

## Abstract

Soft tissue masses are very common and may appear in the context of rheumatic diseases. They usually occur alone but may occasionally be part of the syndromes and can sometimes involve peri-articular tissues. Soft tissue masses can be divided into several categories. In this article, we have categorized them into 3 different groups: (1) pseudotumors, (2) benign tumors, and (3) malignant tumors. Parotid enlargement will also be discussed in this study. The majority of Soft tissue masses are pseudotumors or benign tumors, which can be easily characterized with ultrasound, therefore, considered the first screening tool in the study of this type of lesion. If the tumor is deep or poorly accessible, or present with suspected signs of malignancy, the sonographer may suggest expanding the study with magnetic resonance imaging and/or an ultrasound-guided biopsy of the lesion. Ultrasound is also a good technique for the parotid and submandibular glands and is very useful for evaluating and monitoring Sjogren's syndrome.

**Keywords:** Ultrasound, soft tissue masses, parotid gland, sjögren disease

## Introduction

### Pseudotumors

*Synovial cyst* is a continuation or herniation of the synovial membrane through the joint capsule. The most characteristic one is Baker's cyst. They are associated with joint diseases such as osteoarthritis, inflammatory, and post-traumatic joint diseases.<sup>1</sup> In ultrasound (US), it appears as nodular anechoic lesions with well-defined edges with the typical extension toward the joint (Figure 1).

*Ganglion cyst* is formed by dense connective tissue filled with gelatinous fluid rich in hyaluronic acid and other mucopolysaccharides. Ultrasound may show an ovoid single or poly-lobulated anechoic, well-defined lesion, with no obvious communication with the adjacent joint.

Sonographic compression can be helpful to differentiate a synovial cyst, normally more easily compressible, from a ganglion cyst. Synovial cysts related to active disease might show synovial hypertrophy changing its compressibility, for instance, in a case of a Baker cyst with synovial hypertrophy in rheumatoid arthritis<sup>2</sup> (Table 1) (Figure 2).

*Tenosynovitis* is the inflammation of a tendon and its synovial sheath. In US, it shows an increased thickness and heterogeneity in the echo-structure of the affected tendon, as well as the presence of fluid in its tendon sheath (Figure 3).<sup>3</sup>

*Bursitis* is the inflammation of the small fluid-filled pads, called bursae. Ultrasound shows a collection of well-defined anechoic edges, or with fine echoes inside, in the usual bursa location. Color Doppler (CD) can likewise be used to show signs of infection, such as hyperemia of the bursa and the surrounding tissues (Figure 4).<sup>4,5</sup>

*Rheumatoid nodules* are more common in overlying joint areas such as the metacarpophalangeal, proximal interphalangeal, and metatarsophalangeal (MTP) joints. Nodules appear as oval, generally homogenous (85%), hypoechoic (85%) masses closely attached to the bone surface. The size varies from 2 mm to 5 cm; they are firm, non-tender, and movable in subcutaneous tissue.<sup>6-8</sup>

### ORCID iDs of the authors:

H.C. 0000-0002-7738-6787;  
D.R. 0000-0003-2587-2510;  
V.N. 0000-0002-3635-7672;  
O.C. 0000-0002-4347-3401

**Cite this article as:** Corominas H, Reina D, Navarro V, Camacho O. Ultrasound evaluation of soft tissue masses and parotid gland in clinical rheumatology. *Eur J Rheumatol.* 2024;11(suppl 3):S290-S297.

<sup>1</sup> Department of Rheumatology, Hospital University of Sant Pau, Barcelona, Spain

<sup>2</sup> Department of Rheumatology, Hospital de Sant Joan Despí Moisès Broggi, Barcelona, Spain

Corresponding author:

Vanessa Navarro

E-mail: vane\_nav@hotmail.com

Received: September 14, 2020

Revision requested: September 11, 2021

Last revision received: November 4, 2021

Accepted: November 22, 2021

Publication Date: July 2, 2024

Copyright@Author(s) - Available online at [www.eurjrheumatol.org](http://www.eurjrheumatol.org).

Content of this journal is licensed under a Creative Commons Attribution-NonCommercial 4.0 International License.



*Tophi* are typically in yellow-white color, non-tender, and located within the articular structures, or bursae, and the first MTP joint is the most common but can appear in hands, feet, elbows, and ears.

Sonographically, tophi appear as a heterogeneous mass (80%), composed of hypoechoic and hyperechoic areas, and have poorly defined contours. They can form multiple groups with surrounding anechoic haloes.<sup>7,9,10</sup>

**Benign Tumors**

*Lipoma* is considered the most common soft tissue tumor and is seen in ~2% of the population. They are usually subcutaneous and in US, appear as soft variably echogenic masses. If capsulated, it may be more difficult to identify on US.<sup>11</sup>

When they present a heterogeneous echotexture, more than minimal CD flow or large-size liposarcoma should be suspected. Few authors suggest that a systematic review on the ultrasonography of the soft-tissue lipomas may help to better ascertain the true diagnostic value of this test and that US is a useful tool in the diagnosis of superficial lipomas with good sensitivity and even better specificity and should still be considered the first diagnostic tool option (Figure 5).<sup>12</sup>

*Nodular fasciitis* is typically composed of well-defined, ovoid or lobulated, hypoechoic subcutaneous masses, which may also affect deep muscle fascia.

*Elastofibroma dorsi* has characteristic location (subscapularis) and imaging appearance: US demonstrates a well-defined multi-layered pattern of hypoechoic linear areas of fat deposition intermixed with echogenic fibroelastic tissue (Figure 6).

**Plantar fibromatosis (Ledderhose disease) or palmar fibromatosis (Dupuytren’s disease)** is hypoechoic in US with often a little blurry margination without calcifications or any cystic components, affecting the plantar or palmar fascia, respectively. The lesions may show hypervascularity in a symptomatic phase (Figure 7).

*Tenosynovial giant cell tumors* arise from the tendon sheath. It is unclear whether these lesions represent neoplasms or are merely reactive masses. Ultrasound allows not only the characterization of the lesion but also describes the relationship with the tendon sheath (Figure 8).<sup>13</sup>

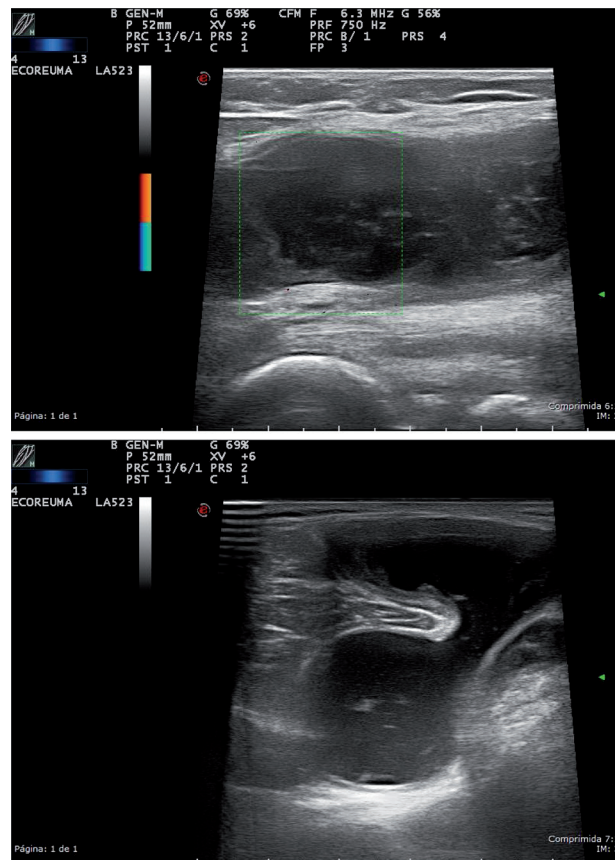


**Figure 1.** High-resolution ultrasound of the knee, in grayscale (longitudinal and transversal) from a patient with popliteal *synovial cyst*. Nodular anechoic lesions with well-defined edges, with a fluid-containing neck between the tendon of semimembranosus and medial head of gastrocnemius.

*Glomus tumor* is usually located in acral areas (typical subungual location). Normally painful under pressure, US shows a hypoechoic lesion with significant Doppler vascularity.<sup>14</sup>

*Hemangiomas* and vascular malformations in US usually present with a defined lesion with markedly heterogeneous echotexture and sometimes contain internal areas,

**Table 1. Ganglion Cyst Versus Synovial Cyst. Ultrasound Characteristics Through a Review of the Literature**

Ultrasound Characteristic and Discriminative Findings	Ganglion Cyst	Synovial Cyst
Compressibility	No	Yes
Location (more frequent)	Wrist, hand, ankle, foot.	Knee (gastrocnemius-semimembranosus bursa) Hip (iliopsoas bursa).
Similar findings		
Blood flow by Doppler evaluation	Absence	Absence or possible
Echogenicity	Anechoic to hypoechoic.	Anechoic to hypoechoic.
Configuration	Uni or multilocular +/- septations	Uni or multilocular +/- septations
Borders	Thin and well defined	Thin and well defined
Joint communication	+/-	+/-
Posterior acoustic shadowing	+/-	+/-

Giard, M., Pineda, C. Ganglion cyst versus synovial cyst? Ultrasound characteristics through a review of the literature. *Rheumatol Int* 35,597–605 (2015). <https://doi.org/10.1007/s00296-014-3120-1>

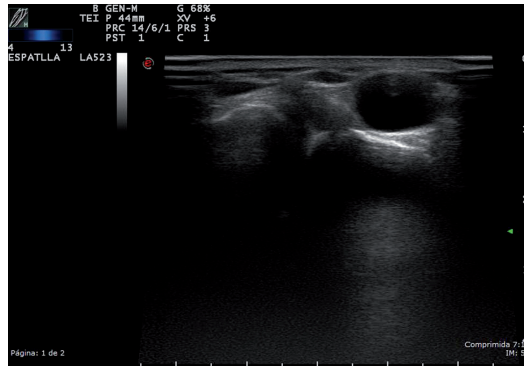


**Figure 2.** High-resolution ultrasound *ganglion cyst* of the acromioclavicular (AC) joint, in grayscale from a patient with swelling at the AC joint; a non-compressible, cystic mass with no obvious communication with the joint, at the site of the swelling.

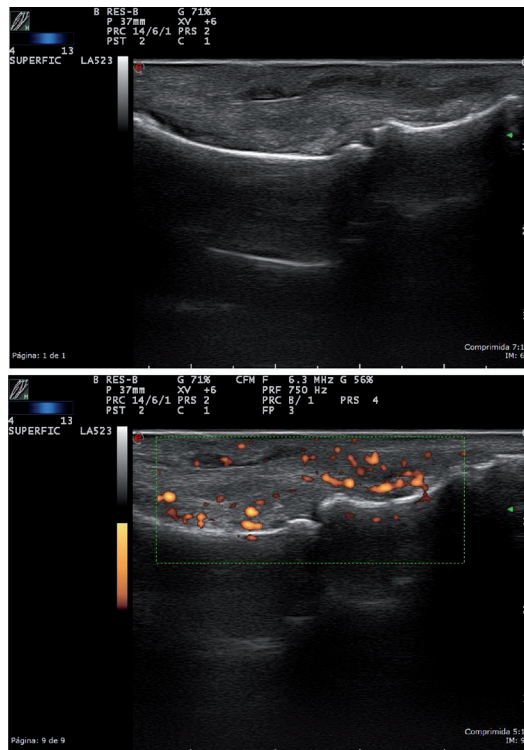


**Figure 3.** High-resolution ultrasound *tenosynovitis* of the hand, in grayscale and color Doppler. The longitudinal scan of the fifth finger flexor tendon shows a thickening tendon sheath with signs of synovial proliferation and increased vascularity.

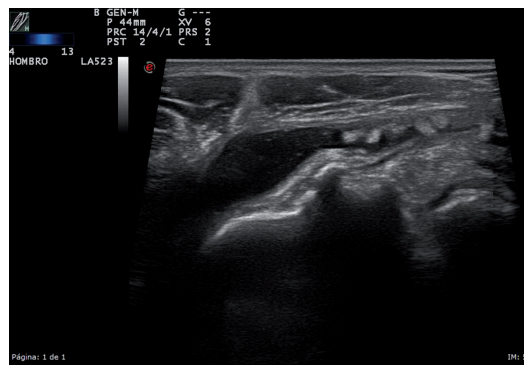


**Figure 4.** High-resolution ultrasound *bursitis* of the shoulder, in grayscale. The longitudinal scan shows the distension of the subdeltoid-subacromial bursitis, with some echoes inside, suggesting microcrystalline disease.

pseudocystic and phleboliths (hyperechoic images with acoustic shadowing). They may have a hyperechoic image (fat) in the periphery of the lesion.<sup>14</sup>

*Schwannomas* are benign tumors of the nerve sheath. Pathognomonic features are the connection with a nerve and the presence of tiny inner pseudocysts. They usually are well vascularized without necrotic areas.<sup>14</sup>

*Neurofibromas* are circumscribed, spindle-shaped defined masses with typically layered appearance in axial scans. In contrast to schwannomas, vascularization is sparse. Multifocal neurofibromas, plexiform and multifocal variants, may occur in neurofibromatosis type 1 disease (Figure 9).<sup>14</sup>

*Myxomas* are the demonstration of a well-defined hypoechoic-anechoic mass surrounding soft tissue and often show a heterogeneous echotexture. Posterior acoustic enhancement may be observed in a significant portion of cases. There may be some internal echoes that are increased through transmission. In ~85% of cases, there is a sonographic bright rim sign of increased echogenicity around the myxoma (i.e., peripheral rim of echogenicity). Frequently, a bright cap sign is seen as a triangular hyperechoic area adjacent to at least one of the poles of the mass. The lesion is hypovascular or avascular on CD US.<sup>15,16</sup>

### Malignant Tumors

**Liposarcoma's** sonographic appearance is large, multilobulated, well-defined isoechogenic/hyperechogenic mass, with tiny hyperechogenic lines and hypervascularity, which might contain nodular or globular foci with echotexture other than adipose tissue.<sup>17</sup>

*Myxoid liposarcoma* represents 20%-50% of all liposarcomas and has an intermediate malignant behavior. Ultrasound appearance reveals a complex, well-defined hypoechoic heterogeneous mass, with solid anechoic non-cystic areas, with posterior acoustic enhancement, that might contain thin septa. Moreover, the Doppler assessment shows hypervascularity surrounding the anechoic areas.<sup>17</sup>

*Dermatofibrosarcoma protuberans* represent 6% of all soft tissue sarcomas and it occurs in males between 20 and 50 years old.<sup>18</sup> The US assessment shows an ovoid or lobulated circumscribed subcutaneous nodule without posterior acoustic enhancement and constitutes a combination of hypoechoic and hyperechoic regions; however, it can appear



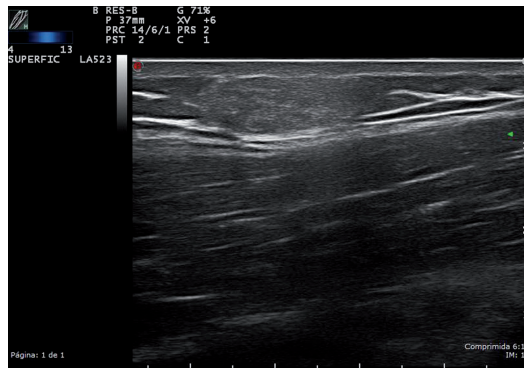


**Figure 5.** High-resolution ultrasound *lipoma* of the right arm in grayscale, in a patient with a soft, slow-growing tumor in the proximal arm. The upper part of the arm was explored: a well-defined, homogeneous, isoechoic oval, superficial lesion of approximately 1.5 cm<sup>2</sup>.



**Figure 6.** A soft tissue tumor was studied in a 60-year-old patient located in the scapular area, which was not painful and appeared on mobilization of the scapula. High-resolution ultrasound in grayscale, of subscapularis zone, demonstrates a well-defined multi-layered pattern of hypoechoic linear areas of fat deposition intermixed with echogenic fibroelastic tissue due to *elastofibroma dorsi*.



**Figure 7.** High-resolution ultrasound in grayscale of the plantar area of the foot in a patient with pain when walking. Ultrasound shows a *plantar fibromatosis* with hypoechoic heterogeneous mass, without calcifications or any cystic components. No hypervascularity was found.

entirely as a hyperechogenic mass. Tiny intral-lesional punctuate non-shadowing echogenic foci may also emerge at the scan evaluation. Typically, it has well-defined contours but may have irregular margins. Power Doppler (PD) shows predominantly hypervascularity in hypoechogenic areas.<sup>19</sup>

Adult *fibrosarcoma* is a rare malignant neoplasm. The US imaging shows a non-specific mass, associated with hypoechogenic and hyperechogenic heterogeneous areas, along with calcifications or ossification, relatively hypovascular, and sometimes may present a pseudocapsule formation with tendency to invade adjacent structures.<sup>20</sup>

*Leiomyosarcoma* is a rare malignant smooth muscle neoplasm that typically occurs in adults. The US scan shows a well-circumscribed oval hypoechogenic mass, with increased posterior enhancement, and may be seen as variable degree of anechoic areas due to necrotic, cystic changes and hemorrhage, with intral-lesional Doppler increased blood flow.<sup>20</sup>

*Rhabdomyosarcoma* is an aggressive malignant striated muscle tumor and it is the most common soft tissue neoplasm of childhood and adolescence. The rhabdomyosarcoma US imaging lacks specificity; can feature a heterogeneous irregular well-defined mass with low to medium echogenicity and may have anechoic irregular areas in zones of necrosis.<sup>21</sup>

*Glomangiosarcoma* or *malignant glomus tumor* is an extremely infrequent soft tissue sarcoma that has high metastatic risk and it is most frequently reported in the lower extremities and in the gastrointestinal tract.<sup>22</sup> Ultrasound characteristics are non-specific, given the lack of cases reported.

*Angiosarcoma*, at US examination, appears predominantly hypoechoic with the increased flow in color and PD imaging, similar to other malignant soft-tissue masses. Heterogeneity areas can be due to hemorrhage.<sup>23</sup>

The malignant peripheral nerve tendon sheath tumor constitutes malignant forms of *neurofibromas* and *schwannomas* and half of them are associated with neurofibromatosis type I, and 11% of them present after post-radiation therapy.<sup>20</sup> Ultrasound cannot distinguish between benign and malignant peripheral nerve sheath tumors, however, is featured as a homogeneous hypoechogenic and fusiform mass with peripheral nerve continuity and posterior acoustic enhancement.<sup>21</sup>

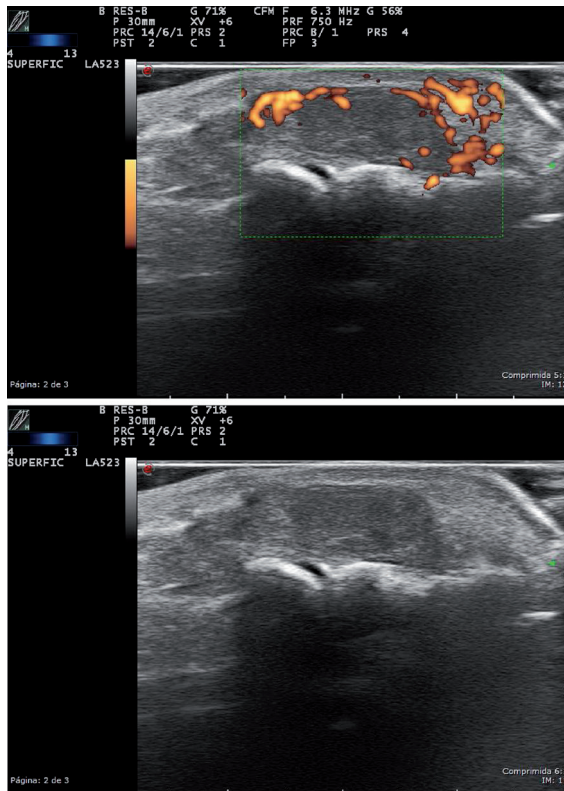


**Figure 8.** High-resolution grayscale and color Doppler ultrasound of the hand, in a young patient with a solitary subcutaneous soft tissue nodule on the volar surface of the second finger. Ultrasound reveals a homogeneous hypoechoic nodule, with hypervascularity, further confirming a tenosynovial giant cell tumors.

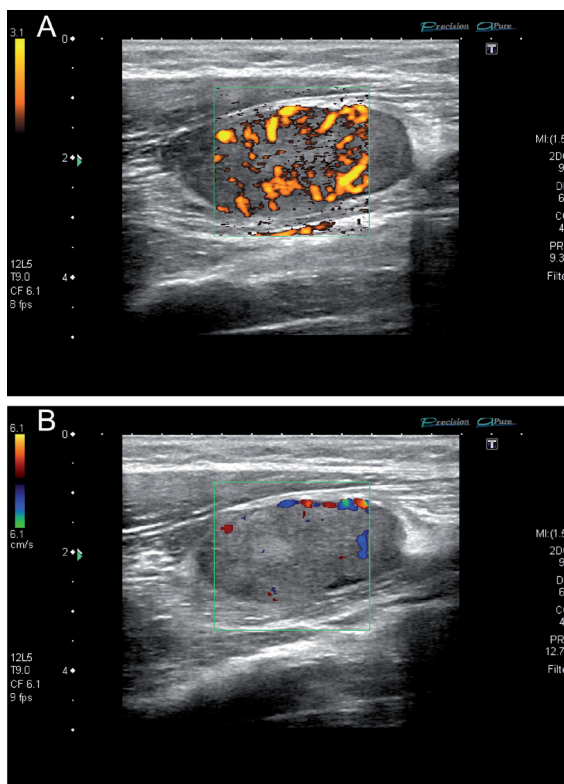


**Figure 9. A, B.** High-resolution grayscale and color Doppler ultrasound of the ankle. Ultrasound reveals a homogeneous, hypoechoic mass of solid appearance, in the posterior tibial nerve due to a neurofibroma.

### Metastases and Lymphomas

The most frequent primary neoplasms which metastasize to muscles are breast carcinomas in woman and lung carcinoma in men. Some metastatic disease rarely affects the skin.<sup>24</sup> Ultrasound imaging has low specificity to show the histologic origin of the tumor but predominantly are well-defined, round or lobular hypoechoic masses with hypervascularity in Doppler assessment.<sup>25</sup> Extranodal lymphoma usually appears in extremities, and US shows a hypoechoic mass, with infiltrative margins and significantly increased vascularity; necrosis is commonly absent (Figure 10).<sup>21</sup>

### Ultrasound of the Parotid and Submandibular Glands in Sjögren's Syndrome

Sjögren's syndrome (SjS) is a systemic autoimmune disease that affects 1-23 people/10 000 inhabitants in Europe and presents with a wide spectrum of clinical manifestations and a profile of specific autoantibodies (Ab).<sup>26</sup> Dryness syndrome dominates the clinical scene and translates an immuno-mediated glandular compromise, accompanied by fatigue, musculoskeletal pain, and a systemic picture in a significant percentage of patients, occasionally complicated by lymphoma in 2%-5% of patients.<sup>27,28</sup>

The diagnosis of the disease is not easy, since different classification criteria have been proposed from the initials of Fox et al.<sup>29</sup> even though the most accepted are the American-European of Vitali et al 2002,<sup>30</sup> with new updates later in 2012 and 2016.<sup>31</sup> None of them has the diagnostic reliability of isolated glandular disease been determined using imaging techniques, such as US. Throughout the history of this disease, an objective and non-invasive technique has been sought to help confirm the diagnosis in a specific way. In 1992, Vitali et al<sup>30</sup> began the study of the application of high-resolution US of the parotid and submandibular glands, with the aim of implementing this technique in clinical practice for the diagnosis of SjS. The authors established a US score for glandular lesion severity with heterogeneous results, summarized in a recent review.<sup>32</sup> Recent works have compared this glandular lesion by US imaging with magnetic resonance imaging and sialography.<sup>33,34</sup> The limitations of these works are the lack of standardization of the technique, which is why Jousse-Joulin et al<sup>35</sup> proposed a consensus on how to standardize the evaluation of key findings by US of the salivary glands and their reliability, which includes: echogenicity,

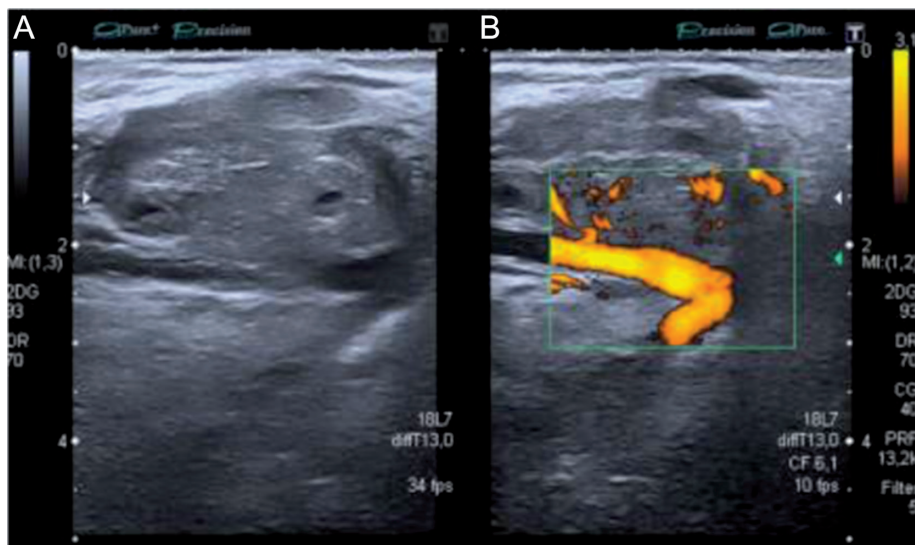


**Figure 10. A, B.** High-resolution grayscale and color Doppler ultrasound of the forearm, in a 53-year-old patient with painless tumor in the front of the forearm, without a history of trauma. A round tumor of less than 1 cm iso/hypoechoic mass in grayscale was observed, moderately delimited, with an attached vessel that nourished the lesion. An important signal Doppler was observed. Due to signs of suspicion, such as heterogeneity, high vascularity, and a very important Doppler signal, an MRI was requested, which showed a well-defined, rounded, 1 cm image, with hypersignal in T1, leading to a metastatic lesion. MRI, magnetic resonance imaging.

**Table 2.** Major salivary gland ultrasonography points and grading method of the submandibular and parotid glands in primary Sjögren Syndrome

	Parotid Glands		Submandibular Glands	
	Left	Right	Left	Right
Echogenicity				
Normal (0); abnormal (fibrosis) 1				
Homogeneity				
Normal (0); abnormal (1)				
Hyperechoic bands				
None (0); <50% of the parenchyma (1); >50% (2)				
Number of hypoechoic/anechoic area (mm)*				
Size of the largest hypoechoic/anechoic areas (mm)**				
Location of the hypoechoic/anechoic areas in the gland				
None (0); isolated (<25% of the surface area) (1); localized (25-50%) (2); scattered (>50%) (3); diffuse (4)				
Number of abnormal lymph nodes in the gland***				
Presence of normal lymph nodes at the upper and / or lower poles of the parotid glands: no (0); yes (1)				
Calcifications				
No (0); yes (1)				
Posterior border visible				
No (0); yes (1)				
Diagnosis advice of pSS based on the seven items				
Ruled out (0); indeterminate (1); ruled in (2)				

Quantitative variables were categorized as follows: \*number of hypoechoic/anechoic areas: none (0), 1-4 (1), >5 (2); \*\*size of the largest area: none (0), <2 (1), >2 (2), \*\*\*abnormal lymph nodes: no (0), yes (1).

Source: Adapted from Jousse-Joulin S et al RMD Open 2017;3:e000364. doi:10.1136/rmdopen-2016-000364. pSS, primary Sjögren's syndrome.

homogeneity, hyperechoic bands, number of hypo/anechoic areas, location of these areas in the gland, number of abnormal lymphoid nodules in the gland, calcifications, visible posterior margin; all in the parotid and submandibular glands bilaterally (Table 2). Based on these US findings, the experts confirmed the diagnostic suspicion, ruled out SjS, or assessed it as undetermined. The final conclusion of this international group was that, after evaluating the reliability of the images, the typical glandular pattern of patients with SjS with an inhomogeneous gland with hypoechoic/anechoic areas in its parenchyma observed on US images could be used by experts in salivary gland US along with the other classification criteria in the diagnosis of SjS concomitantly to reach greater final diagnostic certainty (Figures 11 and 12).<sup>35</sup> However, the US indices described so far present diverse results due to: the heterogeneity of the patients studied, the differences in the US machines used, the different indices, and finally, but not least, that it is a sonographer-dependent technique. Cornec et al.,<sup>36</sup> evaluated the role of glandular US in the diagnosis of SjS, concluding that adding it to the American College of Rheumatology and 2002 classification criteria in clinical practice, sensitivity increases and conversely, the number of biopsies needed decreases, suggesting the performance of biopsies only in those patients with US not suggestive of SjS.

Besides the gray scale and CD US for the diagnosis of SjS, elastography is increasingly offering some structural information about the gland. Elastography is a non-invasive US method that depicts the elasticity and stiffness of the parenchyma to be measured in vivo after deforming stress. It provides a quantitative/qualitative measurement and a dynamic visualization of this tissue stiffness in a wide variety of clinical structures, especially in soft tissue examinations: breast, thyroid, muscle, and salivary gland (Figure 13).

The different elastographic modalities are based on the fact that different pathological processes, which can be inflammatory, fibrotic, or tumor, can cause disturbances in tissue elasticity. As a tool, elastography is reproducible, measures differences in parenchymal stress, and offers high precision in measurements integrated into a color spectrum (elastographic score). At the same time, it obtains pressure ratios in numerical values thanks to specific software. The applicability of elastography in the study of liver, muscle, or breast tissue has been progressively extended, but there are



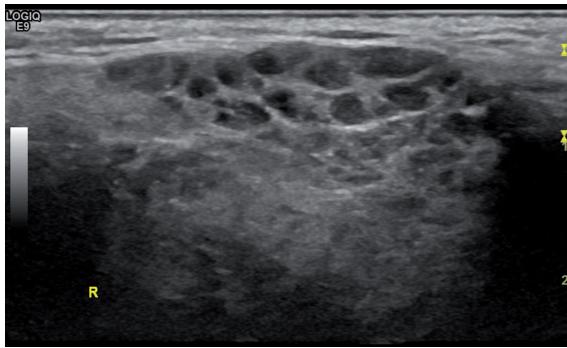


**Figure 11.** Parotid gland: high-resolution ultrasound of the parotid gland (EG) in grayscale from a patient with Sjögren's syndrome. Heterogeneity with numerous hypo/anechoic areas and cystic appearance, without visibility of the posterior border.

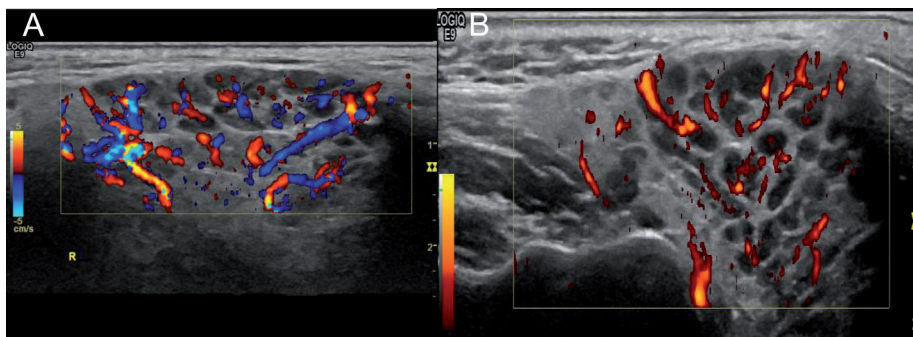


**Figure 12. A, B.** Parotid gland: (A, B) high-resolution ultrasound of the same parotid gland (color Doppler/power Doppler from a patient with Sjögren's Syndrome). Heterogeneity with anechoic, septa, and cystic images with loss of the posterior border.

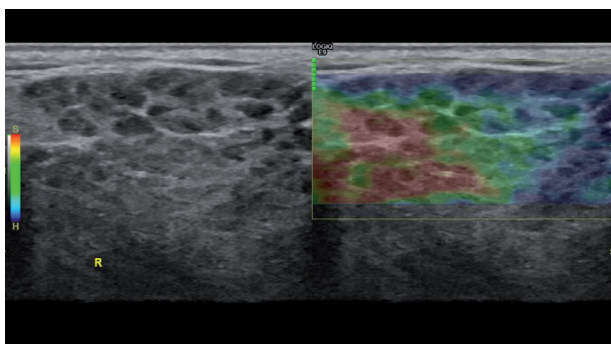


**Figure 13.** Parotid gland: elastography of the right parotid gland from a patient with Sjögren's syndrome. Ultrasound machine with 4D imaging. (GE Logic 9). Heterogeneous density with cystic areas and soft and compressible differentiated focal glandular images (S-red) and rigid non-compressible areas (H-blue).

currently very few studies that have attempted to influence the role that diagnosis of glandular involvement of SjS may have.<sup>37,38</sup>

To summarize, gray scale (EG) and CD or PD US study for the SjS offers detailed information on the structural lesions of the gland according to the currently accepted score.<sup>39</sup> In a short period of time, it will become a necessary tool in the diagnosis and monitoring of patients with SjS since it could be key in improving diagnostic sensitivity, increasing glandular structural definition, describing the inflammatory versus

fibrotic pattern, and improving the monitoring while reducing the number of salivary gland biopsies. Conversely, although elastography is also non-invasive, accessible, and fast, the weakness of preliminary data does not allow us to know the real role it has played so far.

**Peer-review:** Externally peer-reviewed.

**Author Contributions:** Concept – H.C.; Design – D.R.; V.N.; Supervision – H.C.; Literature Review – H.C.; D.R.; V.N.; O.C.; Writing – H.C., D.R., V.N., O.C.; Critical Review – H.C., D.R.

**Declaration of Interests:** The authors declare that they have no competing interest.

**Funding:** The authors declare that this study had received no financial support.

## References

1. Vanhoenacker F, Van Goethem JWM, Vandevenne JE, Shahabpour M. Synovial tumors. *Imaging of Soft Tissue Tumors*. Springer Berlin Heidelberg; 2001:273-300. Accessed September 3, 2020. [https://link.springer.com/chapter/10.1007/978-3-662-07856-3\\_16](https://link.springer.com/chapter/10.1007/978-3-662-07856-3_16).
2. Carra BJ, Bui-Mansfield LT, O'Brien SD, Chen DC. Sonography of musculoskeletal soft-tissue masses: techniques, pearls, and pitfalls. *AJR Am J Roentgenol*. 2014;202(6):1281-1290. [\[CrossRef\]](#)
3. Ray G, Tall MA. Tenosynovitis. *StatPearls*. StatPearls Publishing; 2020. Accessed July 5, 2020. <http://www.ncbi.nlm.nih.gov/pubmed/31335044>.
4. Parker RH. Bursitis. *Clinical Infectious Disease*. 2nd ed. Cambridge: Cambridge University Press; 2015:445-447. Accessed July 5, 2020. <https://www.ncbi.nlm.nih.gov/books/NBK513340/>.
5. Corominas H, Balias R, Estrada-Alarcón P, Reina D, Moya P, Videla M. Giant pes anserinus bursitis: A rare soft tissue mass of the medial knee. *Rheumatol Clin*. 2021;17(7):420-421. [\[CrossRef\]](#)
6. Askari A, Moskowitz RW, Goldberg VM. Subcutaneous rheumatoid nodules and serum rheumatoid factor without arthritis. *JAMA*. 1974;229(3):319-320. [\[CrossRef\]](#)
7. Selim N, Hector C, Benjamin H, Chen Lan X, Ralph SH, Tasanee K. Ultrasonography for assessment of subcutaneous nodules | Request PDF. *The Journal of Rheumatology*. Accessed September 3, 2020. [https://www.researchgate.net/publication/10728252\\_Ultrasonography\\_for\\_assessment\\_of\\_subcutaneous\\_nodules](https://www.researchgate.net/publication/10728252_Ultrasonography_for_assessment_of_subcutaneous_nodules).
8. *Rheumatoid nodules*. UpToDate. Accessed September 3, 2020. <https://www.uptodate.com/contents/rheumatoid-nodules>.
9. Dirken-Heukensfeldt KJM, Teunissen TAM, Van De Lisdonk H, Lagro-Janssen ALM. Clinical features of women with gout arthritis. A systematic review. *Clin Rheumatol*. 2010;29(6):575-582. [\[CrossRef\]](#)
10. De Ávila Fernandes E, Kubota ES, Sandim GB, Mitraud SAV, Ferrari AJL, Fernandes ARC. Ultrasound features of tophi in chronic tophaceous gout. *Skelet Radiol*. 2011;40(3):309-315. [\[CrossRef\]](#)
11. Murphey MD, Carroll JF, Flemming DJ, Pope TL, Gannon FH, Kransdorf MJ. From the archives of the AFIP: Benign musculoskeletal lipomatous lesions. *RadioGraphics*. 2004;24(5):1433-1466. [\[CrossRef\]](#)
12. Rahmani G, McCarthy P, Bergin D. The diagnostic accuracy of ultrasonography for soft tissue lipomas: a systematic review. *Acta Radiol Open*. 2017;6(6). [\[CrossRef\]](#)
13. Middleton WD, Patel V, Teefey SA, Boyer MI. Giant cell tumors of the tendon sheath: analysis of sonographic findings. *AJR Am J Roentgenol*. 2004;183(2):337-339. [\[CrossRef\]](#)

14. ESR, European Society of Radiology. Accessed July 9, 2020. <https://www.myesr.org/>.
15. Petscavage-Thomas JM, Walker EA, Logie CI, Clarke LE, Duryea DM, Murphey MD. Soft-tissue myxomatous lesions: review of salient imaging features with pathologic comparison. *RadioGraphics*. 2014;34(4):964-980. [\[CrossRef\]](#)
16. Girish G, Jamadar DA, Landry D, Finlay K, Jacobson JA, Friedman L. Sonography of intramuscular myxomas: The bright rim and bright cap signs. *J Ultrasound Med*. 2006;25(7):865-869. [\[CrossRef\]](#)
17. Shimamori N, Kishino T, Morii T, et al. Sonographic appearances of liposarcoma: correlations with pathologic subtypes. *Ultrasound Med Biol*. 2019;45(9):2568-2574. [\[CrossRef\]](#)
18. Snow SN, Gordon EM, Larson PO, Bagheri MM, Bentz ML, Sable DB. Dermatofibrosarcoma protuberans: a report on 29 patients treated by Mohs micrographic surgery with long-term follow-up and review of the literature. *Cancer*. 2004;101(1):28-38. [\[CrossRef\]](#)
19. Shin YR, Kim JY, Sung MS, Jung JH. Sonographic findings of dermatofibrosarcoma protuberans with pathologic correlation. *J Ultrasound Med*. 2008;27(2):269-274. [\[CrossRef\]](#)
20. Widmann G, Riedl A, Schoepf D, Glodny B, Peer S, Gruber H. State-of-the-art HR-US imaging findings of the most frequent musculoskeletal soft-tissue tumors. *Skelet Radiol*. 2009;38(7):637-649. [\[CrossRef\]](#)
21. Stramare R, Beltrame V, Gazzola M, et al. Imaging of soft-tissue tumors. *J Magn Reson Imaging*. 2013;37(4):791-804. [\[CrossRef\]](#)
22. Abu-Zaid A, Azzam A, Amin T, Mohammed S. Malignant glomus tumor (glomangiosarcoma) of intestinal ileum: a rare case report. *Case Rep Pathol*. 2013. [\[CrossRef\]](#)
23. Gaballah AH, Jensen CT, Palmquist S, et al. Angiosarcoma: clinical and imaging features from head to toe. *Br J Radiol*. 2017;90(1075). [\[CrossRef\]](#)
24. Corominas H, Estrada P, Reina D, Cerdà-Gabaroí D. Ultrasonography as a diagnostic tool for skin metastasis of a prostate adenocarcinoma. *Rheumatol Clin*. 2016;12(1):54-56. [\[CrossRef\]](#)
25. Park SB, Kang BS. Value of ultrasonographic evaluation for soft-tissue lesions: focus on incidentally detected lesions on CT/MRI. *Jpn J Radiol*. 2017;35(9):485-494. [\[CrossRef\]](#)
26. Brito-Zerón P, Baldini C, Bootsma H, et al. Sjögren syndrome. *Nat Rev Dis Primers*. 2016;2:16047. [\[CrossRef\]](#)
27. Díaz-López C, Geli C, Corominas H, et al. Are there clinical or serological differences between male and female patients with primary Sjögren's syndrome? *J Rheumatol*. 2004;31(7):1352-1355.
28. Birt JA, Tan YM, Mozaffarian N. Sjögren's syndrome: managed care data from a large United States population highlight real-world health care burden and lack of treatment options. *Clin Exp Rheumatol*. 2017;35(1):98-107.
29. Fox RI, Robinson CA, Curd JG, Kozin F, Howell FV. Sjögren's syndrome. Proposed criteria for classification. *Arthritis Rheum*. 1986;29(5):577-585. [\[CrossRef\]](#)
30. Vitali C, Bombardieri S, Jonsson R, et al. Classification criteria for Sjögren's syndrome: a revised version of the European criteria proposed by the American-European Consensus Group. *Annals of the Rheumatic Diseases*. BMJ Publishing Group; 2002;62:554-558. Accessed July 4, 2020. [www.annrheumdis.com](http://www.annrheumdis.com).
31. Shiboski CH, Shiboski SC, Seror R, et al. American College of Rheumatology/European League Against Rheumatism classification criteria for primary Sjögren's syndrome: a consensus and data-driven methodology involving three international patient cohorts. *Arthritis Rheumatol*. 2016;69(1):35-45. Accessed July 4, 2020. [/pmc/articles/PMC5650478/?report=abstract](https://pubmed.ncbi.nlm.nih.gov/27111111/).
32. Luciano N, Ferro F, Bombardieri S, Baldini C. Advances in salivary gland ultrasonography in primary Sjögren's syndrome. *Clin Exp Rheumatol*. 2018;36(5):159-164.
33. Baldini C, Zabotti A, Filipovic N, et al. Imaging in primary Sjögren's syndrome: the "obsolete and the new." *Clin Exp Rheumatol*. 2018;36(3):215-221.
34. Niemelä RKN, Takalo R, Pää E, et al. Ultrasonography of salivary glands in primary Sjögren-Sjögren's syndrome. A comparison with magnetic resonance imaging and magnetic resonance sialography of parotid glands. *Rheumatology*. 2004;43:875-879. Accessed July 4, 2020. <https://academic.oup.com/rheumatology/article-abstract/43/7/875/2899091>.
35. Jousse-Joulin S, Nowak E, Cornec D, et al. Salivary gland ultrasound abnormalities in primary Sjögren's syndrome: consensual US-SG core items definition and reliability. *RMD Open*. 2017;3(1):e000364. [\[CrossRef\]](#)
36. Cornec D, Jousse-Joulin S, Pers JO, et al. Contribution of salivary gland ultrasonography to the diagnosis of Sjögren's syndrome: toward new diagnostic criteria? *Arthritis Rheum*. 2013;65(1):216-225. [\[CrossRef\]](#)
37. Cindil E, Oktar SO, Akkan K, et al. Ultrasound elastography in assessment of salivary glands involvement in primary Sjögren's syndrome. *Clin Imaging*. 2018;50:229-234. [\[CrossRef\]](#)
38. Klauser AS, Miyamoto H, Bellmann-Weiler R, Feuchtner GM, Wick MC, Jaschke WR. Sonoelastography: musculoskeletal applications. *Radiology*. 2014;272(3):622-633. [\[CrossRef\]](#)
39. Hofauer B, Mansour N, Heiser C, et al. Sonoelastographic modalities in the evaluation of salivary gland characteristics in Sjögren's syndrome. *Ultrasound Med Biol*. 2016;42(9):2130-2139. [\[CrossRef\]](#)